Environmental Science and Pollution Research (2022) 29:15800–15815
https://doi.org/10.1007/s11356-021-16889-6

RESEARCH ARTICLE

Immune responses, DNA damage and ultrastructural alterations of gills in the marine mussel *Lithophaga lithophaga* exposed to CuO nanoparticles

Amina E. Essawy[1] · Soheir S. El sherif[1] · Gamalat Y. Osman[2] · Rehab M. El Morshedy[1] · Abir S. Al-Nasser[3] · Sherin K. Sheir[2]

Received: 16 February 2021 / Accepted: 30 September 2021 / Published online: 11 October 2021

Abstract

Nanoparticle (NP) pollution is a worldwide problem. Copper oxide nanoparticles (CuO NPs) are one of the most used NPs in a variety of applications, which results in their increased release into the marine environment. In the present work, the marine mussel *Lithophaga lithophaga* was used as a model organism to evaluate the toxic effects of CuO NPs following 28 days of exposure to sub-lethal concentrations (5 and 20 µg/L). The time points were 1 day of exposure to assess the cell viability, phagocytosis in mussel haemocytes and genotoxicity (DNA damage in gills), 1, 14 and 28 days of exposure to evaluate copper concentrations in water and gills, as well as metallothionein concentration in gills, while gill histology and SEM examination were done after 28 days of exposure. The results indicated that the accumulation of CuO NPs in gills increased with concentration and time. Mussel exposure to CuO NPs increased neutral red uptake. However, the phagocytic abilities decreased in haemocytes with increased concentration. CuO NPs caused DNA damage in the gills even at low concentrations (5 µg/L). CuO NPs caused histopathological alterations in gills, such as brown cell accumulation, necrosis, dwarfism of filaments and ciliary erosion. In conclusion, exposure of the mussel *L. lithophaga* to CuO NPs led to concentration- and time-dependent responses for all the examined biomarkers. Thus, *L. lithophaga* may be used as a bioindicator organism in the assessment of CuO NP toxicity.

Keywords Immune responses · Genotoxicity · Scanning electron microscopy · Histology

Introduction

The European date mussel *Lithophaga lithophaga* is an endolithic bivalve that inhabits carbonate rocks (limestone). It is endemic to the Mediterranean Sea on hard substrates of the upper sub- and mid-littoral zones (D'Angelo and Gargiullo 1978). The date mussel *L. lithophaga* was the subject of several studies of its biology, population dynamics, fecundity and habitat (Galinou-Mitsoudi and Sinis 1995; Gonzalez et al. 2000; Devescovi 2009).

Heavy metal concentration has not been thoroughly analysed on the Egyptian Mediterranean coast. Heavy metal (Cr, Pb, Ni, Zn, Cu, Mn) concentration in the sediments has been investigated (Okbah et al. 2014) in addition to the chemical composition of the Egyptian Mediterranean coast, focusing on metals such as Mg and Br (Nessim et al. 2010). However, there are no references concerning NP concentrations in the Egyptian Mediterranean coast yet.

CuO NPs are used in many applications, such as batteries, semiconductors and inks, photovoltaic cells, pigments in ceramics, hospital equipment, fabrication of solar cells and filtration materials of air and liquid (Mortimer et al. 2010; Dasari et al. 2013; Almeida et al. 2019). Specifically, CuO NP uses in marine antifouling, medical applications and environmental remediation could affect the marine environment (Anyaogu et al., 2008; Singh et al. 2015; Ghadimi et al. 2020).

Communicated by Bruno Nunes.

✉ Sherin K. Sheir
sherin.sheir@yahoo.com

[1] Zoology Department, University of Alexandria, Alexandria, Egypt

[2] Invertebrates Division, Zoology Department, University of Menoufia, Shibin el Kom, Egypt

[3] Department of Biology, Faculty of Sciences, University of Jeddah, Jeddah, Saudi Arabia

The vast utilization of CuO NPs resulted in their increased release into the environment, especially the marine ecosystem. The understanding of CuO NP toxicity on different biomarkers of marine benthic filter feeders is still unclear (Dasari et al. 2013; Alnashiri 2015). Bivalves have been used for the assessment of NP toxicity due to (i) their filter-feeding ability, which is responsible for the filtration of large volumes of water, as well as (ii) the processes of the phagocytosis and endocytosis performed by the epithelial tissues of the digestive gland, the mantle, the gills and the haemocytes which accumulate large amounts of NPs (Moore, 2006; Canesi et al. 2012).

Several biomarkers have been used to detect the effects of NPs on aquatic bivalves. NPs target the immune functions in bivalve molluscs and induced immunomodulation in the freshwater mussel, *Elliptio complanata* (Gagné et al. 2008). Zha et al. (2019) investigated the immunomodulation effects of NPs (ZnO, Fe_2O_3, CuO and multi-walled carbon nanotube (MWCNT)) in the blood of the clam, *Tegillarca granosa*. The results showed that exposure to the tested NPs reduced the total haemocyte counts, altered the haemocyte composition and constrained the phagocytic activities of haemocytes. Also, antioxidants and metallothioneins (MTs) were affected in the gills and digestive gland of the bivalve species *Scrobicularia plana*, after 21 days of exposure to 10 µg/L CuO NPs (Mouneyrac et al., 2014). Gomes et al. (2013) showed that CuO NP (10 µg/L) exposure increased DNA damage in the mussel haemocytes of *Mytilus galloprovincialis* after 2 weeks of exposure. The induction of MTs, a cysteine-rich protein that binds metals and contributes to metal detoxification and sequestration, was reported in various aquatic species under laboratory metal exposure (Amiard et al. 2006). MT induction was detected throughout the exposure of the gills of the mussel *Mytilus galloprovincialis* to CuO NPs (Gomes et al. 2011 and 2014a). Ruiz et al. (2015) reported various histopathological alternations in the gills of *M. galloprovincialis* after 21 days of exposure to CuO NPs, such as haemocytic infiltration and brown cell aggregation. Al-bairuty (2013) indicated that exposure to Cu NPs increased the incidence of oedema, lamellar fusion, clubbed tips, hyperplasia and necrosis in the secondary lamellae of the gill filaments of the rainbow trout.

The main objective of the present study was to investigate the toxicological impacts of exposure to CuO NPs in the gills of date mussel, *L. lithophaga*, using different immunological, genetic and histological biomarkers**.**

Material and methods

Collection of mussels and stock aquaria

The mussels *L. lithophaga* were collected from Elanfoshy bay in Alexandria, Egypt (February 2019, Fig. 1, lat. 31.205753 N and long. 29.924526 E). Three hundred mussels were carefully collected and immediately transferred to a cool box containing seawater. The animals were conveyed to the laboratory at Alexandria University, Faculty of Sciences, within 3 h. All mussels were kept for 7 days in aerated filtered seawater to ensure acclimatization to the laboratory conditions. Stock animals were fed twice a week using 1 mL/L microalgae mix (*Chlorella* sp. and *Nannochloropsis* sp., 25,000 cells/mL).

Experimental design

Ninety mussels were divided into 3 groups: 10 tanks/group, 3 mussels/tank. The mussels' biometrics were length (6.60 ± 0.85 cm), width (2.29 ± 0.25 cm) and weight (12.10 ± 2.29 g). All tanks were acid-washed (10% HNO3) and rinsed in clean seawater before use. Each tank (radius 9 and height 17 cm) contained 1 L of filtered seawater. Five,

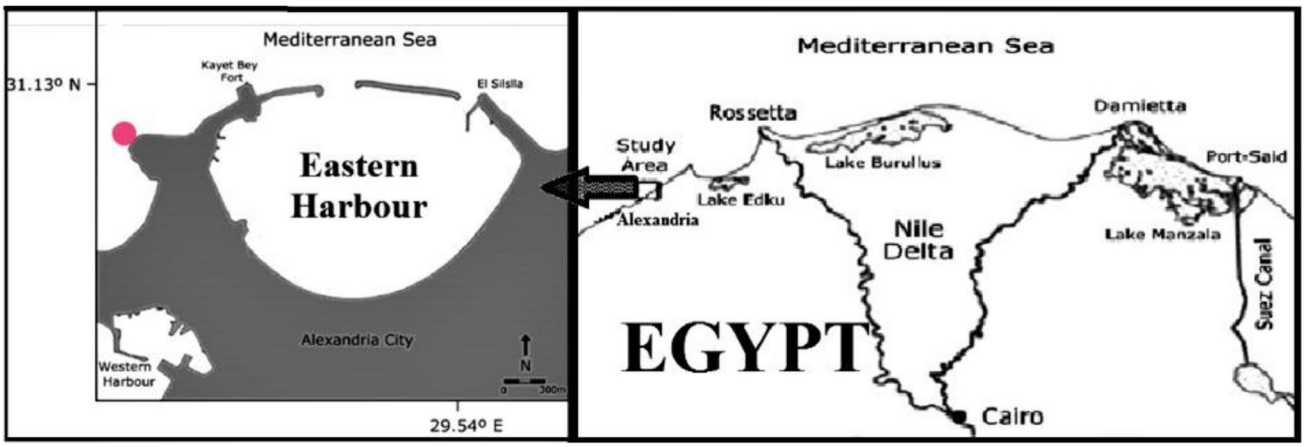

Fig. 1 A map showing lower Egypt, Alexandria city and El Anfoshy bay (red circle), the collection site of *L. lithophaga* mussels

10, 15 and 20 µg/L concentrations of CuO NPs according to Mouneyrac et al. (2014) and Alnashiri (2015) were chosen. A quality control experiment was run using the previous concentrations for 28 days for toxicity/mortality evaluation. Because there was no mortality recorded during the quality control experiment (sublethal concentration), the lowest and the highest concentrations of CuO NPs were chosen for the main experiment, i.e. 5 and 20 µg/L CuO NPs for conc. effect comparison on the selected biomarkers. Mussels were exposed to 0, 5 and 20 µg/L of CuO NPs for 28 days as the main experiment. Tanks were re-dosed every 48 h with CuO NPs, after a 100% water exchange. Total Cu concentrations were measured in the tanks on sampling days (1, 14 and 28, Table 1). The seawater parameters measured were temperature (17–20 °C), salinity (38.8–42.3‰), ammonia (0.02–0.03 mg/L), pH (7.2–7.6), conductivity (58.4–62.9 ms/cm), total dissolved solids (37.5–48.4 g/L) and dissolved oxygen (8–9.6 mg/L).

Cu accumulation and MT concentration were measured in the gills on sampling days (1, 14 and 28). Mussel samples were collected after 1 day of exposure in order to assess DNA damage in gills via comet assay, while the immune functions of haemocytes were assessed through phagocytosis and neutral red uptake. At the end of exposure (28 days), gills were dissected for SEM and histological examination.

Characterization and analysis of CuO NPs

CuO NPs were prepared in the Chemistry Laboratory, Faculty of Science, Alexandria University, and according to the procedure of Zhu et al. (2011) from copper acetate. For the preparation of the stock solution, 600 mL of 0.2 M copper acetate solution and 2 mL of glacial acetic acid (CH_3COOH) were mixed and boiled with stirring. Afterwards, 30 mL of 8 M sodium hydroxide was added to the previous solution. The colour of the solution changed from blue to black and a black suspension was formed simultaneously. The reaction was carried out under continuous stirring and boiling for 2 h. The final mixture was cooled to room temperature and centrifuged to get wet CuO precipitate. The wet precipitate was washed twice with distilled H_2O to remove the impurity ions. CuO nanofluids of different size fractions were obtained by re-dispersing the wet precipitate into different amounts of distilled water under ultrasonic vibration (120 W, 40 Hz). NPs were characterized to establish particle/agglomerate/aggregate size and shape analyses. Particles were suspended in distilled water and were analysed using transmission electron microscopy (JEM-1400 Plus electron microscope, Japan), Alexandria University. The size, shape and charge of CuO NPs were characterized by X-ray diffraction (XRD) analysis using a powder diffractometer (Bruker, Germany), ultraviolet analysis using UV/visible spectrophotometer (Helios alpha, Unicam) and zeta potential using Zetasizer NanoZS (Malvern Instruments Ltd, Malvern, UK). Total Cu in water was measured using atomic absorption spectrometry (Thermo Scientific S SERIES, AA Spectrometer).

Table 1 CuO NP concentrations in seawater samples of different groups after the experimental time points

Time points	Seawater concentrations		
	Control	5 µg/L	20 µg/L
1 day	ND	5.084 ± 0.061*	20.178 ± 0.489*$
2 weeks	ND	5.125 ± 0.343*	20.168 ± 0.296*$
4 weeks	ND	5.045 ± 0.077*	20.092 ± 0.763*$

Note: $n = 5$. Data were expressed as mean ± S.D. as µg/L. *Represented significant difference between control and exposed groups. $Represented a significant difference between the exposed groups when $p \leq 0.05$. *ND* not detected

CuO NP accumulation in the gills

CuO NPs were analysed according to Federici et al. (2007) with minor modifications. Briefly, approximately 0.05 g of fresh tissue ($n = 5$ mussels/concentration) was oven-dried, weighed and digested in 1 mL of concentrated nitric acid (HNO_3). The mixture was heated at the water bath at 70 °C until the mixture was clear. Then, the digest was diluted with distilled water to reach 5 mL. CuO NP accumulation was measured using atomic absorption spectrometry (Thermo Scientific S SERIES, AA Spectrometer).

Immunological assays

Two standard assays were performed on haemocytes: neutral red uptake (NRU) and phagocytosis assays after 1 day of exposure to CuO NPs. Haemolymph was withdrawn from the control and exposed mussels ($n = 5$ mussels/concentration) using a 1-mL syringe, placed into Eppendorf tubes and stored on ice (Sheir and Handy 2010).

Neutral red assay

This assay was performed according to Babich and Borenfreund (1992). The assay measures neutral red uptake by haemocytes, which is used as a general indicator of cell health and viability. Thirty microlitres of Neutral Red solution (NR) and samples were added into the wells ($n = 5$ mussels/concentration). Samples were incubated in a 0.004% NR solution for 3 h. The excess NR solution was removed using physiological saline. Then, the remaining cells were lysed with 200 mL of acidified ethanol. Then, the plate was read using a plate reader (Seac, Radim Company, Italy) at 550 nm (Sheir et al. 2013).

Phagocytosis assay

Yeast cells were used as target cells for phagocytosis by haemocytes of the mussel, *L. lithophaga*. The stock solution was prepared in PBS to obtain a concentration of 10,000 cells/mL. The monolayer technique described by Abdul-Salam and Michelson (1980) was used to determine the phagocytic index of haemocytes. Freshly collected haemolymph from mussels (100 µL) was overlaid with an equal volume of yeast suspension on a clean glass slide and stained with Giemsa. Prepared slides were microscopically examined using a light microscope (Optica, Italy). The phagocytic index was calculated as a percentage of positive haemocytes from the calculated 100 cells/concentration and triplicate/concentration.

Comet assay

DNA damage was measured in gills after 1 day of exposure using a single-cell gel electrophoresis technique (comet assay) according to Singh et al. (1988). Crushed gill samples ($n = 5$ mussels/concentration, 0.5 g) were transferred to 1-mL ice-cold PBS. TBE buffer (pH 13) was added to the samples for 15 min. The cell suspension (100 µL) was mixed with 600 µL of low melting agarose (0.8% in PBS). The coated slides were immersed in lysis buffer (0.045 mol/L Tris/Borate/EDTA, pH 8.4) containing 2.5% sodium dodecyl sulphate for 15 min. The slides were then placed in an electrophoresis chamber containing the same TBE buffer, but without SDS and run at 2 V/cm and 100 mA for 2 min. The slides were stained with ethidium bromide at 4 °C. Ethidium bromide–stained DNA using a × 40 objective on a fluorescence microscope [with excitation filter 420–490 nm linked to a camera (Olympus)] was used for visualization of DNA damage. DNA damage was evaluated using the Olive tail moment and the percentage of DNA in the tail (% DNA tail) from 50 cells in each sample (triplicate/treatment) using a computer-based image analysis system (OpenComet v 1.3).

Metallothionein analysis

Metallothionein concentration in gills was determined using MT ELISA kit (Catalogue No. CSB-EQ027262FI, Cusabio) on days 1, 14 and 28 according to Viarengo et al. (1997) as a protein. Samples ($n = 5$ mussels/concentration) were immediately stored at − 20 °C. All reagents, working standards and samples were prepared according to the instructed protocol. The optical density of wells was measured within 5 min, using a microplate reader at 450 nm.

Scanning electron microscopy

For scanning electron microscope studies, gills from different groups were fixed in 2% glutaraldehyde and 0.05 M cacodylate buffer (pH 7.4) for 2 h at 4 °C. The tissue was post-fixed in 1% osmium tetroxide in the same buffer for 1 h at 4 °C and rapidly washed in cacodylate buffer. The specimens were dehydrated in graded ethanol at room temperature, critical point dried and gold-coated according to standard procedures (Felgenhauer 1987). The prepared specimens were examined and photographed at the desired magnifications using a JSM-IT200 series (Japan) scanning electron microscope.

Histology

Histological examinations were carried out at the end of the experimental time (28 days). Mussels were removed from their shells ($n = 5$ mussels/concentration), and the whole gill lamellae were carefully collected and fixed in 10% buffered formaldehyde for 24 h. Samples were dehydrated in an ascending series of alcohol (50–100%), cleared in triplicate xylene changes and embedded in melted paraplast at 60 °C. Sections (5–8 mm thickness) were cut and stained with haematoxylin and eosin (Romeis 1989). Gills from controls and exposed mussels were processed together in batches for histology to eliminate artefacts between treatments. Fifteen slides/group and three slides/mussel were examined and photographed using light microscopy (Olympus LC20, Germany). The width of the gill axis, filaments and interfilamentar spaces were measured in micrometres, and the mean for each section was derived by randomly counting more than five replicates from a randomly selected area on a section from each mussel. Histological alterations were analysed and scored for control and exposed mussels as a percentage (%) of the total collected sections.

Statistical analysis

All data were analysed using Statgraphics Centurion XVI Plus software with a rejection level of $P \leq 0.05$. All data are expressed as the means ± standard deviation (SD) for mussels ($n = 5$) per treatment. Data were analysed using one-way ANOVA for concentrations effects. In all analyses, a variance check was performed using Bartlett's test, and the default multiple range test (least-squares difference, LSD test) was used to locate specific treatment and time effects within ANOVAs. Data were analysed using a two-way analysis of variance (two-way ANOVA) for the interaction between concentrations and time effects.

Results

Characterization of CuO NPs

The particle size, shape, distribution and charge of CuO NPs were analysed using a transmission electron microscope (TEM), ultraviolet, zeta potential and X-ray diffraction as illustrated in Fig. 2. The particle sizes measured by TEM ranged in diameter from 6.63 to 23.90 nm and tend to aggregate in the medium (Fig. 2a). X-ray diffraction analysis showed that CuO NPs have a monoclinic crystal structure (Fig. 2b). The pattern demonstrated two main diffraction peaks which are attributed to main crystal phases in HKL (− 1, 1, 1) and (1, 1, 1) with the largest intensities. So, the synthesized crystalline powder is a single-phase structure. The average size crystallite size was within the range of 10–13 nm as determined by the XRD peak broadening technique (Scherrer' equation, Xpowder12 V. 2018.01.01 software). A Zeta sizer for surface potential was used to evaluate the surface charge of CuO NPs. It recorded a negative charge (− 21.1 ± 3.95 mV), which confirmed CuO NPs have a good degree of stability and indicated decreased droplet coalescence due to the large electrostatic repulsion between CuO NPs (Fig. 2c). The UV–Vis absorption spectrum of the prepared CuO NPs with particle size 10–12 nm (calculated from XRD spectrum) shows an absorption peak's position at 291 nm, as shown in Fig. 2d (left). The absorption spectrum was used to calculate the optical energy gap of the prepared CuO NPs through Tauc's formulas (Tsunekawa et al. 2000). Figure 2d (right) represents $\alpha h\upsilon^2$ versus $h\upsilon$ plot of the absorption spectrum. The energy band gap of the CuO NPs was estimated by fitting a straight line to the linear part of the curve and the value of the optical gap is the intercept with the line of the $h\upsilon$ axis. The obtained direct band gap value was 3.78 eV for our sample. This value was larger than 3.2 eV of the bulk CuO NPs as reported previously by Koffyberg et al. (1982). This increase in the direct band gap value toward the blue value and decrease in NP size was attributed to the quantum confinement effect.

Bioaccumulation of CuO NPs in *L. lithophaga* gills

Either the absence of CuO NPs or traces of them were detected in the gills of the control mussels during the experimental period. The concentration of CuO NPs in the gills after 14 days of exposure was significantly higher in the 20 µg/L exposed group ($p = 0.005$) than the control and the 5 µg/L exposed group. The highest concentrations of CuO NPs in the mussel gills were recorded in the 20 µg/L exposed group after 28 days ($p = 0.003$, Table 2). The bioaccumulation of CuO NPs in the gills of exposed mussels was concentration- and time-dependant ($p = 0.000$, two-way ANOVA).

Effects of CuO NPs on immunological responses of *L. lithophaga*

Neutral red uptake (NRU) and phagocytic activity in the mussel haemocytes were measured after 1 day of exposure to 5 and 20 µg/L CuO NPs (Fig. 3). NRU in haemocytes of the mussels showed the lowest values in the control group (0.066 ± 0.037) and the highest values in the 20 µg/L exposed group (0.126 ± 0.034). The group exposed to 5 µg/L had a value of 0.102 ± 0.004, indicating an increase of NRU in comparison with the haemocytes of the control group, which was not however statistically significant ($p > 0.05$). The present results showed a significant ($p = 0.009$) increase in NRU in the haemocytes of mussels exposed to 20 µg/L CuO NPs compared to the control group.

As far as the phagocytic activity analysis is concerned, the cytoplasm of the control haemocytes was light purple, and the pseudopodia of the haemocytes showed spreading with several branches of each pseudopodium, ranging from 2 to 7 branches. The cytoplasm of the haemocytes from the 5 µg/L CuO NP-exposed mussels was a darker purple compared to the control group and the pseudopodia of the haemocytes showed less branching. The cytoplasm of the haemocytes from the mussels exposed to 20 µg/L CuO NPs was a lighter purple compared to the control group and the haemocytes presented blunt pseudopodia with the minimum branches of 1–2 per/haemocyte (Fig. 4).

The phagocytic activity of exposed mussels significantly ($p \leq 0.05$) decreased when compared to the control mussels. The percentages of phagocytic and non-phagocytic cells in the control group were 59.6 and 40.4%, respectively. The mussels exposed to 5 µg/L CuO NPs recorded 17.5 and 82.4% phagocytic and non-phagocytic haemocytes, respectively. However, in mussels exposed to 20 µg/L CuO NPs, phagocytic and non-phagocytic haemocyte percentages were 13.1 and 86.9%, respectively (Fig. 4d).

According to the number of phagocytic yeast cells, 59.6% of haemocytes from the control group phagocytosed at least one yeast cell. The spreading pseudopodia of the haemocytes with ingested yeast cells was highly observed in this group (Fig. 4a, d). The number of yeast cells phagocytosed by haemocytes reached up to 19 ± 2.0 yeast cells/haemocyte in the control group. Only 17.5% of the haemocytes in the 5 µg/L exposed group had the phagocytic ability and the number of yeast cells phagocytosed by haemocytes reached 13 ± 1.7 yeast cells/haemocyte (Fig. 4b, d). Notably, haemocytes from the 20 µg/L exposed group had the lowest phagocytic ability. Only 13.1% of haemocytes were able to phagocytose yeast cells

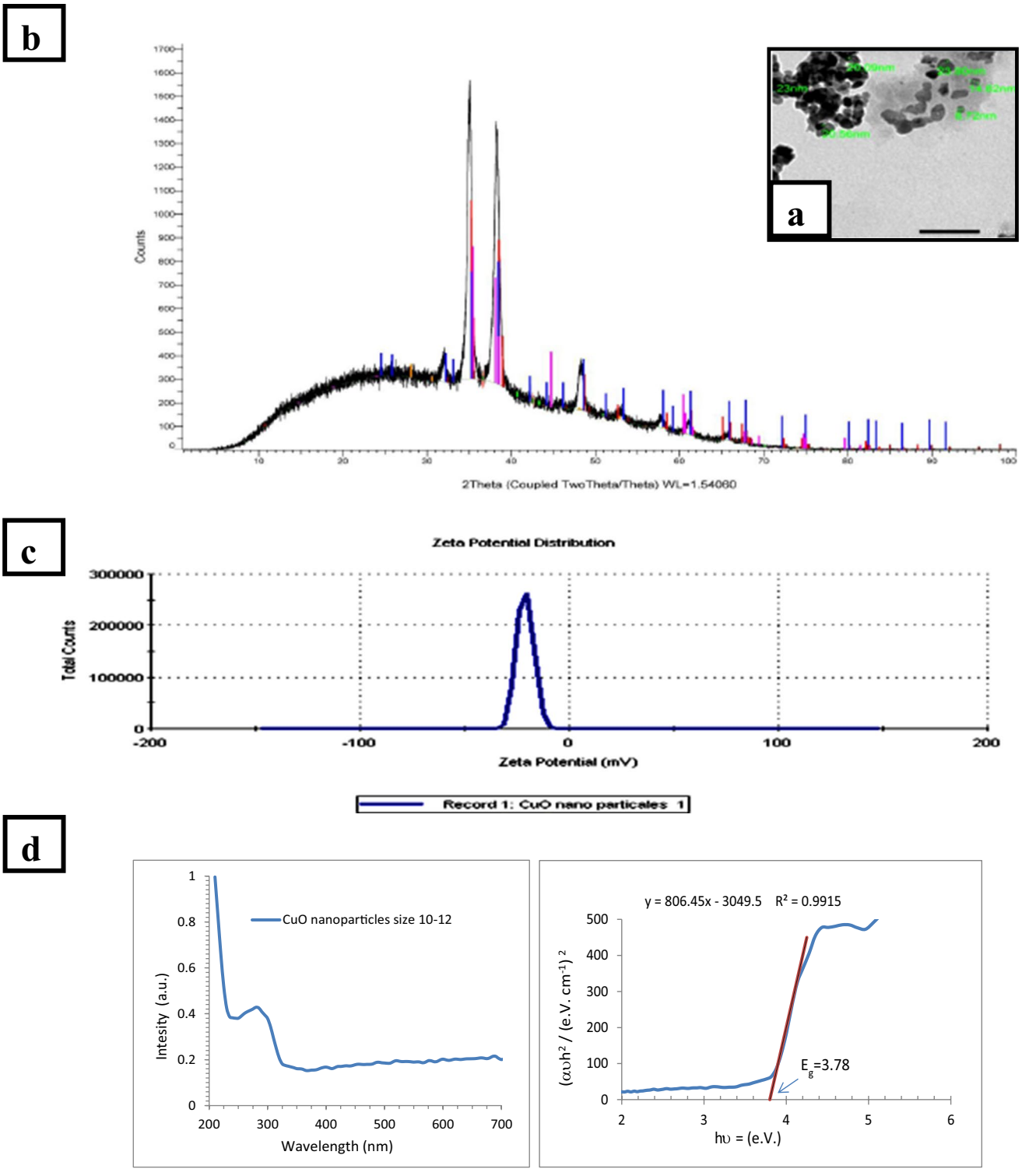

Fig. 2 Characterization of CuO NPs using **a** a transmission electron microscope, scale bar 100 nm; **b** X-ray diffraction (XRD); **c** zeta potential (ζ); and **d** UV–visible absorption spectrum (left) and direct band gap estimation (by Tauc's formula) for CuO NPs of size 10–12 nm (right)

and the number of yeast cells phagocytosed by haemocytes reached 9 ± 1.1 yeast cells/haemocyte (Fig. 4c, d).

Effect of CuO NPs on DNA integrity of *L. lithophaga* gills

DNA damage in the gills of mussels after 1 day of exposure was determined using the comet assay, and the results are shown in Fig. 5. A significant increase ($p \leq 0.05$) of up to threefold of DNA damage in the gills of mussels exposed to different concentrations of CuO NPs was observed compared to the control group. The tail length was the lowest in the control group (1.18 ± 0.11 µm), followed by the 5 µg/L exposed group (1.92 ± 0.47 µm), and the longest was in the 20 µg/L exposed group (3.42 ± 0.29 µm). The DNA tail % also showed the lowest values in the control group (7.99 ± 1.64%), followed by the 5 µg/L exposed group (13.28 ± 1.84%), and the highest value was observed in the 20 µg/L exposed group (16.12 ± 1.69%). The tail moment showed the lowest values in the control group, followed by the 5 µg/L exposed group, and the highest values in the 20 µg/L exposed group (0.36 ± 0.06, 0.87 ± 0.27 and 1.76 ± 0.36 arbitrary units, respectively). The olive tail moment was 0.68 ± 0.09 in the control group, followed by 1.46 ± 0.28 in the 5 µg/L exposed group and 2.09 ± 0.19 in the 20 µg/L exposed group ($p = 0.02$).

Table 2 CuO NP concentrations in gills of *L. lithophaga* mussels collected from the control and exposed groups after the experimental time points

Time points	Control	5 µg/L	20 µg/L
1 day	ND	0.038 ± 0.007 *	0.069 ± 0.009 *$
2 weeks	0.001 ± 0.001	0.778 ± 0.084 *	1.151 ± 0.432 *$
4 weeks	0.002 ± 0.002	1.064 ± 0.135 *	1.939 ± 0.731 *$

Note: $n = 5$. Data were expressed as mean ± S.D. as µg/g. *Represented significant difference between control and exposed groups. $Represented a significant difference between the exposed groups when $p \leq 0.05$

Effects of CuO NPs on metallothionein concentrations of *L. lithophaga* gills

Metallothionein concentrations in the gills of mussels after 1, 14 and 28 days are presented in Table 3. A significant increase ($p = 0.001$), up to tenfold, in MT concentrations was observed in the mussels exposed to different concentrations of CuO NPs and different time points. MT concentrations ranged from 0.812 ± 0.013 to 1.02 ± 0.836 pg/mL in the control group, and they ranged from 2.15 ± 0.047 to 3.66 ± 0.167 pg/mL in the 5 µg/L exposed group. However, the highest value of 10.6 ± 0.393 pg/mL was reached in the mussels exposed to 20 µg/L CuO NPs. MT concentrations in the gills of exposed mussels were exposure- and time-dependant ($p = 0.000$, two-way ANOVA).

Effects of CuO NPs on gill morphology of *L. lithophaga*

Scanning electron microscope (SEM) investigation of the control group showed that gill lamellae were composed of numerous, parallel, regularly arranged filaments. Each lamella has a large, wide and flat axis with three types of cilia according to Dufour and Beninger (2001) and Riisgård et al. (2015). The first type was the frontal cilia, which are found on the upper surface of the filament. The second type was the abfrontal cilia, which were arranged alongside the frontal cilia. The third type was the lateral cilia, which

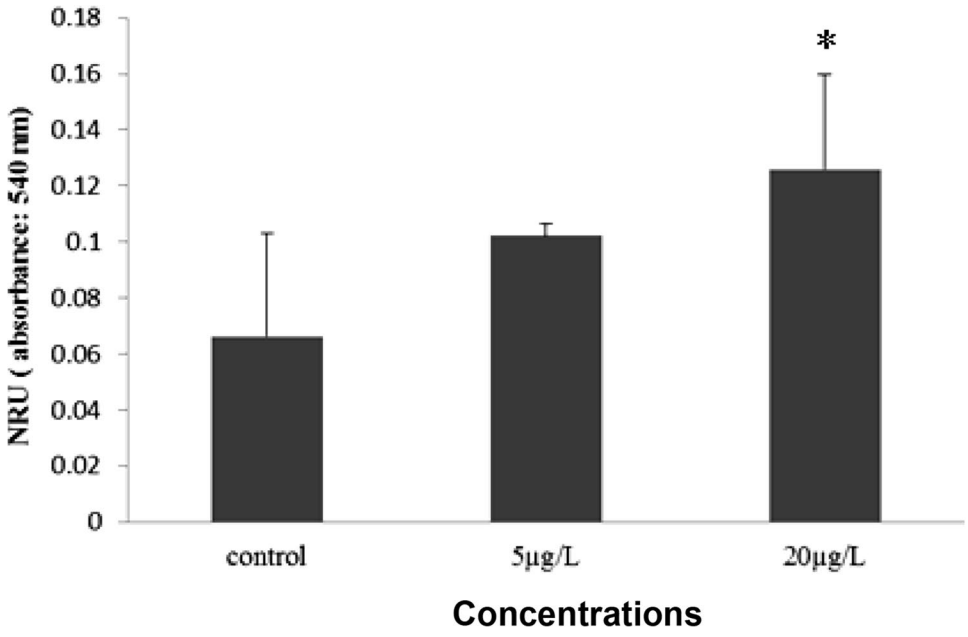

Fig. 3 Effect of CuO NPs on the NRU in the heamolymph of mussels after 1 day of exposure. Data were expressed as mean ± S.D. *A significant difference between control and exposed group when $p \leq 0.05$

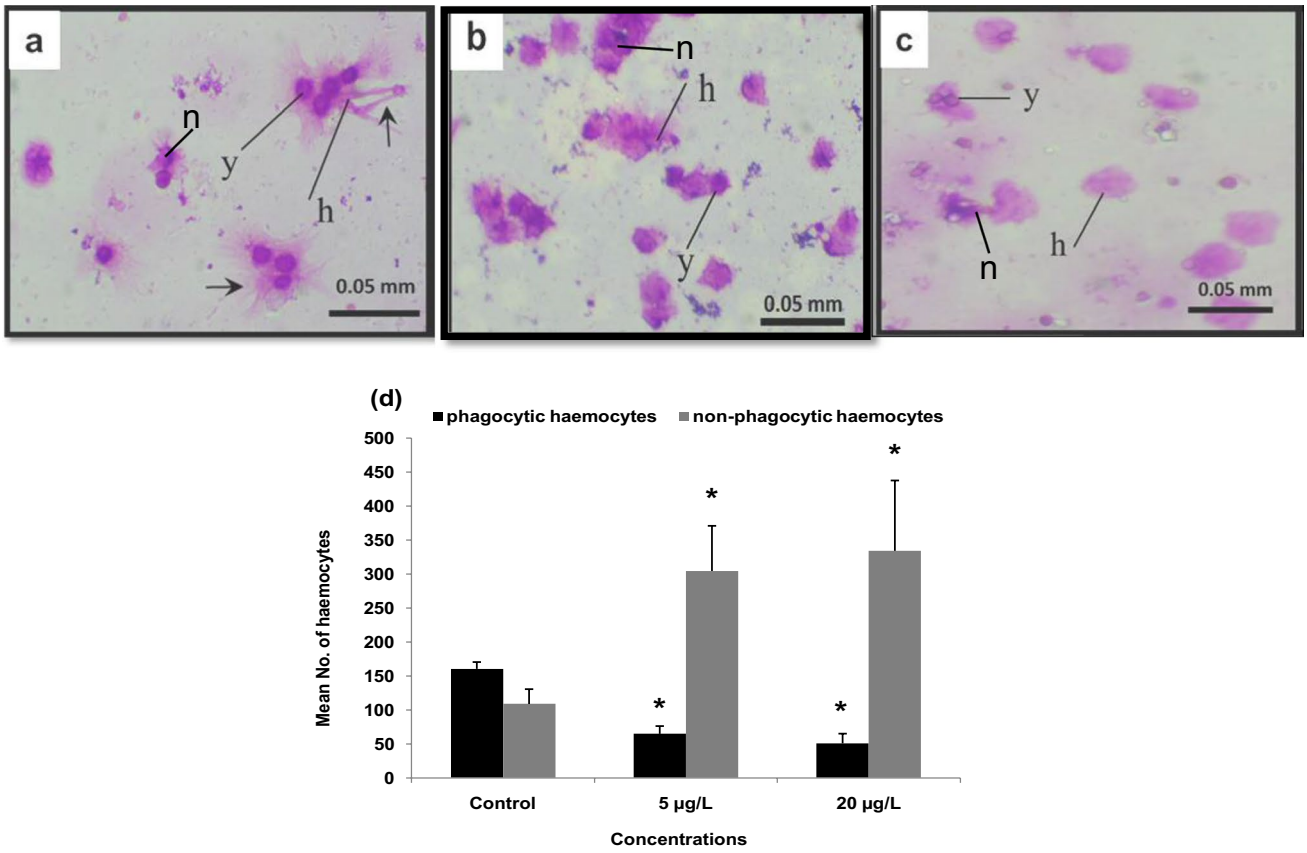

Fig. 4 Light micrographs of haemocytes (stained with Giemsa) showing **a** the phagocytic activity of haemocytes in the control group showing active phagocytosis and branched pseudopodia of haemocytes and **b**, **c** the phagocytic activity of haemocytes of 5 and 20 µg/L CuO NPs exposed groups, respectively, after 1 day of exposure showing less activity of phagocytosis and less or no branched pseudopodia of haemocytes. h, hemocyte; y, yeast cells; n, nucleus; arrows, branched pseudopodia of haemocytes. **d** A histogram showing the phagocytic activity (%) in the control and exposed mussels' haemocytes to 5 and 20 µg/L CuO NPs. *A significant difference between control and exposed groups; $A significant difference between the exposed groups, when $p \leq 0.05$

exhibited a noticeable very long thick latero-frontal cirri and ramification at the tip (Fig. 6a, e).

Examination of *L. lithophaga* gills exposed to 5 µg/L CuO NPs for 28 days revealed obvious alterations. The gill axis was significantly smaller than the control axis (645.5 ± 0.5 µm, $p \leq 0.001$) and measured approximately 301.0 ± 2.0 µm in width. A significant decrease ($p = 0.0001$) in the filament width (30 ± 0.6 µm) was observed when compared to the control group (40.4 ± 0.5 µm). The interfilamentar spaces were significantly increased ($p = 0.0002$, 4.2 ± 0.2 µm) in width in the 5 µg/L CuO NP group when compared to the control group (3.0 ± 0.5 µm). Although all types of cilia exhibited

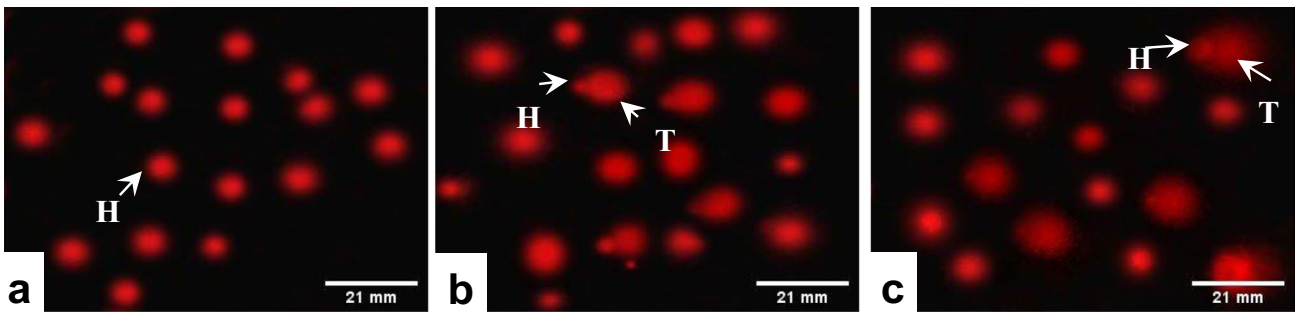

Fig. 5 Single-cell electrophoresis assay showing the effect of CuO NP exposure on gills of the mussel *L. lithophaga* after 1 day **a** control group, **b** and **c** showing DNA damage in gills of mussels from 5 and 20 µg/L CuO NPs exposed groups, respectively. H, head; T, tail

Table 3 Effect of CuO NPs on metallothioneine concentrations in gills of *L. lithophaga* mussels

Time points	MTs (pg/mL)		
	Control	5 µg/L	20 µg/L
1 day	0.812 ± 0.013	2.150 ± 0.047*	6.644 ± 0.199*$
2 weeks	0.920 ± 0.025	2.544 ± 0.051*	8.400 ± 0.574*$
4 weeks	1.020 ± 0.836	3.660 ± 0.167*	10.600 ± 0.393*$

Note: $n = 5$. Data were expressed as mean ± S.D. *Represented significant difference between control and exposed groups. $Represented a significant difference between the exposed groups when $p \leq 0.05$

normal morphology and density, the cilia were irregularly arranged with CuO NP precipitates (Fig. 6b, d, f, g) and numerous CuO NPs were seen scattered and precipitated on the gill axis surface as shown in Fig. 6 (d and d`).

SEM analysis of gills taken from *L. lithophaga* mussels exposed to 20 µg/L CuO NPs for 28 days showed severe alterations compared to the lower concentration. Gill filaments were irregularly arranged with more curvatures. The filaments appeared significantly ($p < 0.001$) smaller than the control gills and measured 26.0 ± 2.0 µm in width. The gill axis appeared highly convoluted and smaller with marked cilia and microvilli erosion on the lower edge of the axis, and numerous CuO NPs were found scattered on its surface. The gill axis was smaller in width than the control gill axis and measured approximately 270.3 ± 0.6 µm. Significantly wider interfilamentar spaces (10.5 ± 0.5 µm width, $p < 0.001$) were observed in several parts of the gill lamellae. Ciliary erosion was also observed, and the gill filaments appeared almost naked of cilia in some parts, while in other parts, the frontal surface had very rare ciliary discs that were frontally situated as disposition. In addition, composite cilia were laterally situated in an abnormal position and structure (Fig. 6c, h).

Effects of CuO NPs on the histological structure of *L. lithophaga* gills

A longitudinal section through the gill lamellae of the control *L. lithophaga* showed the long parallel gill filaments that were nearly 9.33 ± 0.66 µm in length and 40.5 ± 0.5 µm in width at its widest point and 32.83 ± 1.16 µm across its frontal arrow tip. The adjacent filaments were joined together laterally along their length by obvious regular ciliary junctions called ciliary discs. The distance between the adjacent filaments was approximately 17 ± 0.5 µm at the lateral region and 10.83 ± 0.16 µm at the abfrontal region. The branchial vessel internal width was 11.2 ± 1.2 µm and passed through the middle of each filament and was filled with haemocytes. It was lined with a chitinous sheet that supported the external epithelial cell layer of the gill filament. The chitin sheet varied in thickness, ranging from 2.0 ± 0.5 µm beneath the lateral gill epithelium to 3.8 ± 0.2 µm at the abfrontal and frontal tips (Fig. 7a).

The histological observation of the gills from *L. lithophaga* exposed to 5 µg/L CuO NPs for 28 days showed shorter filaments, with a severe shrinkage in the length (4.4 ± 0.26 µm). The width of the gill filaments decreased ($p < 0.05$) and reached 21.5 ± 0.5 µm at the widest point at its tip. The distance between the adjacent gill filaments was wider than the control group and measured approximately 32 ± 2 µm at the lateral region and 16.83 ± 1.16 µm at the abfrontal region (arrow pointed edge). Erosion of the frontal and lateral cilia in some places and dilation in the branchial vessel in some places were also observed. The chitinous sheet thickness proportions changed completely and had the same thickness at all parts of the gill filament (2.0 ± 0.5 µm in width). Gill epithelia in the abfrontal part lost its normal integrity, structure and cilia. Some scattered nuclei of the necrotic epithelial layer and vacuolization were observed in damaged areas (Fig. 7b, cand Table 4).

Histopathological alterations were noticed in the longitudinal section of the gill filaments of *L. lithophaga* exposed to 20 µg/L CuO NPs for 28 days. The gill filaments showed a decrease ($p = 0.01$) in length (2.16 ± 0.16 µm) when compared to the control filaments. An irregularity of all gill filaments and an increase ($p < 0.05$) in the thickness of the chitinous sheets, especially at the frontal parts forming a characteristic bulge (51 ± 2.0 µm), were recorded. The width of some filaments in the lateral region varied from 17 ± 0.5 to 42.8 ± 1.16 µm. The interfilamentar spaces were widened to reach 42.0 ± 2.0 µm at the lateral region when compared to the control gills (40.5 ± 0.5 µm) and 21.8 ± 1.2 µm at the abfrontal region (frontal bulge). Complete erosion of the frontal and lateral cilia in this group was noted, and the ciliary junctions were completely absent. The epithelial layer also appeared necrotic along some of the gill filaments. Dilation in the branchial vessel was also observed in some places and reached 35.5 ± 0.5 µm in width. However, some filaments appeared highly constricted to the extent that they completely blocked the branchial vessel. The chitin sheet varied in thickness from approximately 4.0 ± 0.5 µm beneath the lateral gill epithelium to 11.2 ± 1.2 µm at its frontal and abfrontal parts. More severe alterations in the histoarchitecture of the filaments were observed, such as gill atrophy, branchial dysmorphia and necrotic gill filaments. Detached epithelial cells were observed in the abfrontal region, and the lateral region of filament had a highly thickened gill epithelium that was deeply stained and had enlarged epithelial cells. Haemocyte infiltration was detected in the gill axis and parts of the gill filaments. A large number of brown cells in the lumen of the branchial vessel was also noted (Fig. 7d, e and Table 4).

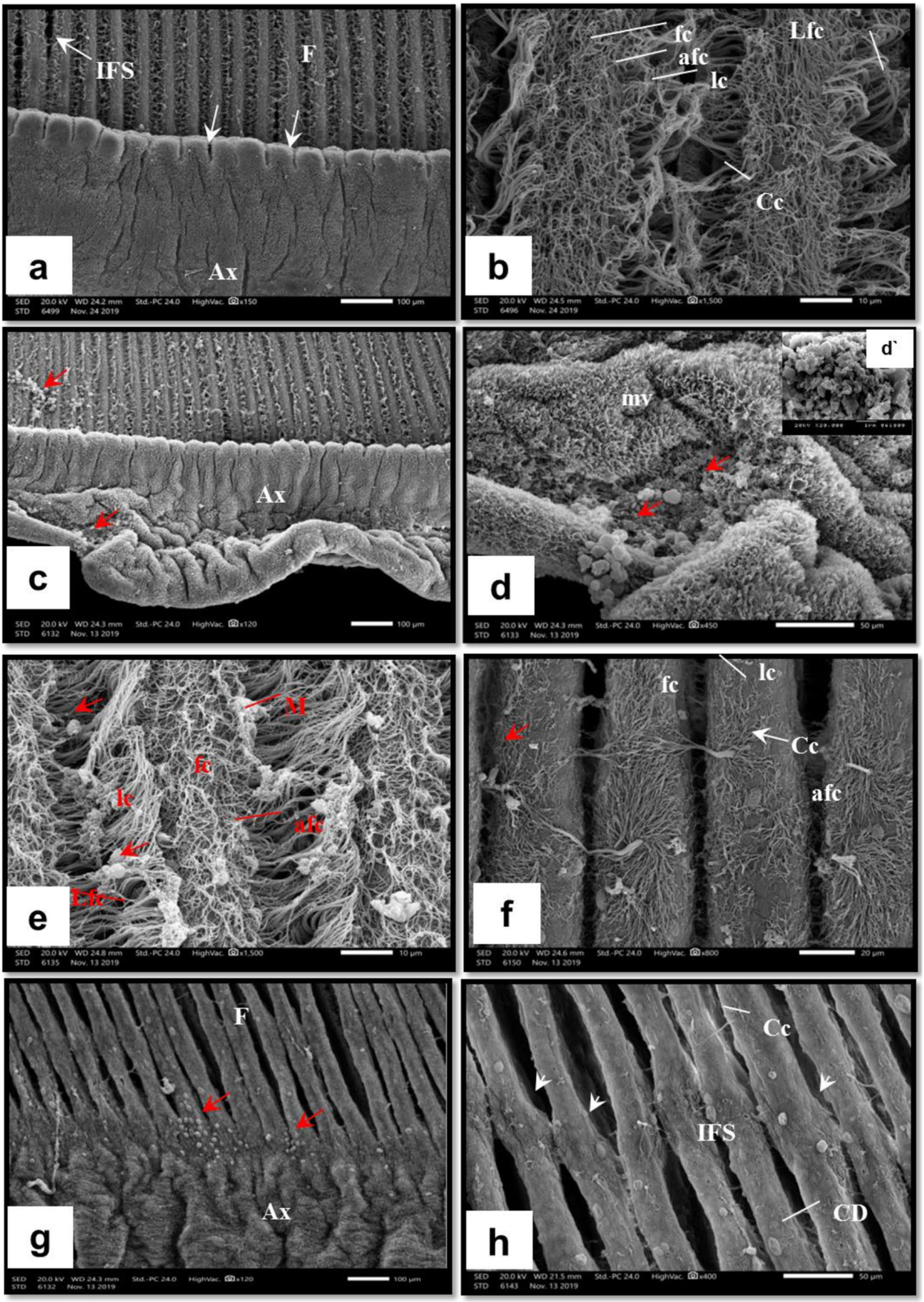
IFS
F
Ax
a
fc
afc
lc
Lfc
Cc
b
Ax
c
mv
d`
d
M
fc
lc
afc
Lfc
e
fc
lc
Cc
afc
f
F
Ax
g
Cc
IFS
CD
h

◂**Fig. 6** Scanning electron micrographs of *L. lithophaga* gills exposed to CuO NPs showing **a**, **b** control group, **c**–**f** 5 µg/L CuO NPs exposed group, **g** and **h** 20 µg/L CuO NPs exposed group, **a** gill filaments (F) axis (Ax), interfilamentar space (IFS), edge of the axis (arrows). **b** The upper surface of the filament is covered with frontal cilia (fc), abfrontal cilia (afc), long lateral cilia (lc), latero-frontal cirri (Lfc) and composite cilia (Cc). **c** Shrinked axis, NPs. **d** Shrinked edge of axis with many microvilli (mv) and numerous CuO NPs and **d`** showing SEM photograph of CuO NPs. **e** Illustrating different types of cilia. **f** Gill filaments with irregularly arranged cilia and increase mucus secretion (M). Numerous CuO NPs. **g** Ciliary erosion and mucus secretion. **h** Altered gill filaments with degenerated composite cilia and frontal cilia, ciliary disks (CD) at the frontal surface and larger inter filament space were observed

Discussion

The obtained data of CuO concentration in gills' tissue showed increased bioaccumulation with the increase of exposure time and concentration of CuO NPs. The mussels exposed to 20 µg/L CuO NPs accumulated more CuO NPs than the 5 µg/L exposed ones. Gomes et al. (2011) recorded a predominant accumulation of CuO NPs in the gills of the mussel, *M. galloprovincialis*. Many authors reported that metal nanoparticles accumulated mostly in the gills of bivalves (Canesi and Corsi 2016; Van Den Brink et al. 2019). Notably, CuO has quite different dissolution potentials, and there are some reports that the toxicity of CuO NPs may be partially related to dissolution (Gunawant et al. 2011). The present CuO NPs were characterized as having a nearly quantum confidant size, with a negatively charged surface. The NP negative charge could enhance their cellular uptake and render them more toxic than positively charged particles. According to Holsapple et al. (2005), the shape and size of NPs could influence their toxicity, the site of deposition, fate and clearance from the body. They added that quantum confinement could lead to size-dependent electro-optical phenomena of the particles. Also, the smaller the particles, the larger the number of atoms found on the surface. The surface charges of the particles have a huge effect on their interaction with proteins and biological fluids. This will affect the interaction between the cell components and the particles. The toxicity and ability of NPs to enter the cells increase with their decreasing size (Tedesco et al. 2008 on *M. edulis* and Liu et al. 2014 on the lung cells).

The current results recorded immunotoxic effects of CuO NPs on the mussel haemocytes, demonstrating a significant increase of NRU and inhibition of phagocytic activity after 24 h of exposure. Neutral red retention by haemocytes is an indicator of the integrity of the lysosomal system in the cell (Lowe et al. 1995), which indicated lysosomal instability under the effects of CuO NPs in the present study. Toxicants compromised the energy sources of the mussel haemocytes and indirectly affected the phagocytosis process since it is an energy-dependant function (Luengen et al. 2004). Zha et al. (2019) investigated the effects of CuO NPs on the haemocytes of the clam, *Tegillarca granosa*, and found reduced total cell counts, altered cell composition, constrained phagocytic activities of the haemocytes and down-regulation of the immune-related genes. They suggest that NP exposure hampered the immune responses of clam haemocytes most likely via three pathways: (1) induction of reactive oxygen species, which causes DNA damage and reduces the cell viability of haemocytes; (2) alteration of the in vivo contents of neurotransmitters; and (3) affecting the expression of immune- and neurotransmitter-related genes. Hu et al. (2014) confirmed that CuO NPs decreased the lysosomal stability of *M. edulis*. CuO NPs caused toxic effects at the organelle level of subcellular organization (Koehler et al. 2008). In addition, CuO NPs found to be more immunotoxic to the haemocytes of mussels than the ionic Cu which make it a specific biomarker for immunotoxicity (Katsumiti et al. 2018).

The present study showed that DNA damage in gills increased significantly after 24 h of CuO NP exposure. Earlier works reported similar findings of CuO NP-induced DNA damage in haemocytes of the mussel, *M. galloprovincialis*, and the clam, *Tegillarca granosa*, using comet assay (Gomes et al. 2013; Zha et al. 2019). The damage of DNA in haemocytes was a result of increased oxidative stress in the exposed bivalves. The dissolution and release of ions from the nanoparticles, oxidative stress and DNA damage are the major modes of action of engineered nanomaterials (ENMs) in bivalves, and these factors are directly or indirectly mediated by reactive oxygen species and free radical production (Canesi et al. 2010; Gomes et al. 2013; Rocha et al. 2015). ENMs penetrate the nuclear membrane via its pore complexes because of their small size and promote DNA damage by direct interaction with DNA or nucleic acids due to high reactivity and surface charge following the intracellular release of ionic metals or via the overproduction of ROS, which led to oxidative damage (Gomes et al. 2013).

The current study showed a significant increase in MT concentration in the gills of the exposed mussels to CuO NPs in a time- and concentration-dependent manner. Nanoparticle exposure induced defence response mechanisms, such as MT production, since MTs are involved in metal detoxification (Van et al. 2005; Marquis et al. 2009). In addition, the uptake of metals varies significantly depending on the species and environmental factors as mentioned by Luoma and Rainbow (2005). According to Gomes et al. (2014b), Ag NPs (10 µg/L) were more effective in MT induction in the gills rather than the digestive gland of the mussel, *Mytilus galloprovincialis.* CuO NPs induced MTs in the gills of the mussel *M. galloprovincialis* and showed a linear induction with the time and concentration of CuO NPs, which was directly related to Cu accumulation in the mussels after

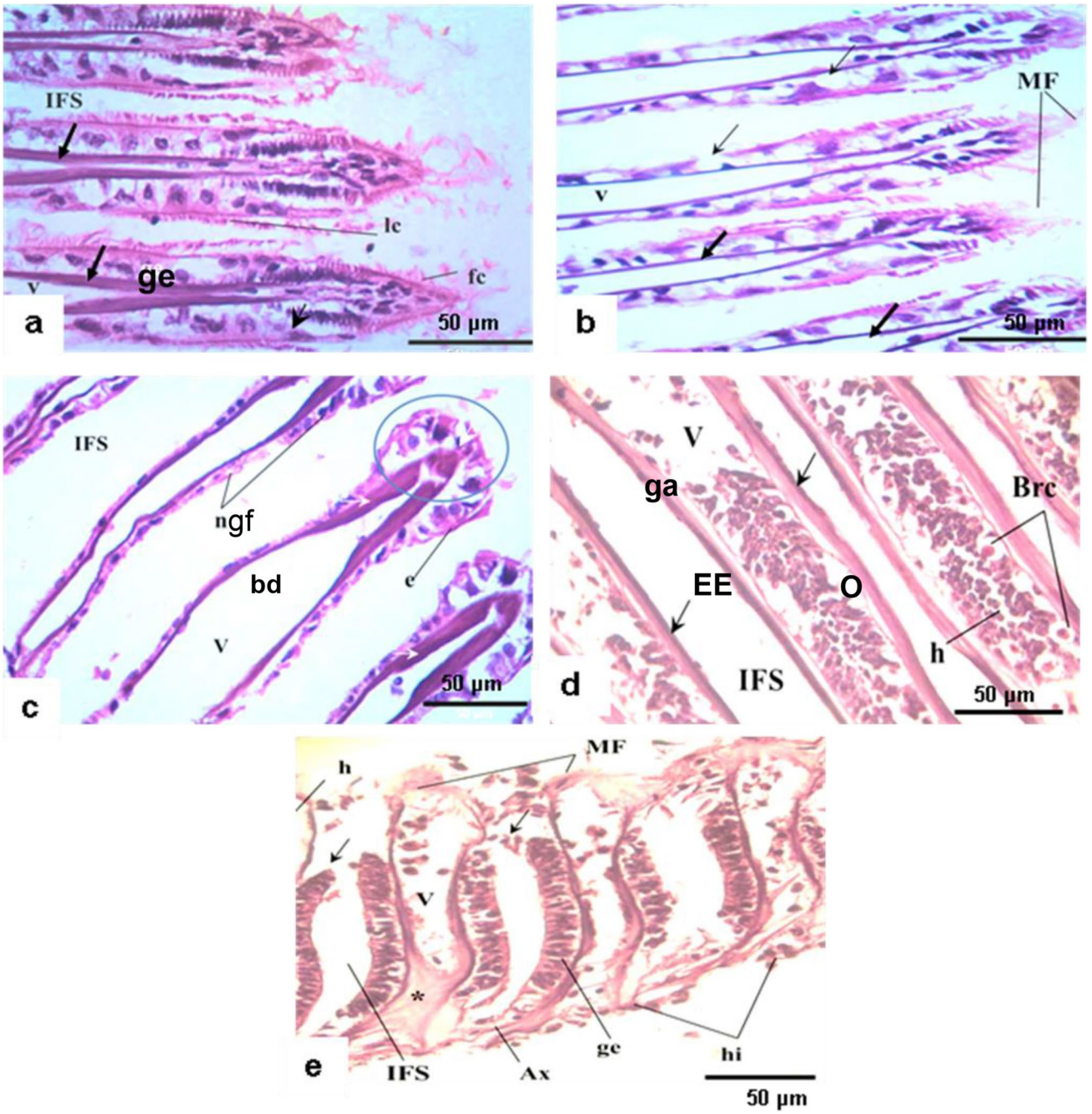

Fig. 7 Light micrographs of sections through the gills of *L. lithophaga* exposed to CuO NPs stained with haematoxylin/eosin showing the (**a**) control group, **b**, **c** 5 µg/L CuO NPs exposed group, **d**, **e** 20 µg/L CuO NPs exposed group. Gill filaments (F), branchial vessel (v), chitinous sheet (white arrows), increased inter filament space (IFS), (fc) frontal cilia, (lc) lateral cilia, (ge) gill filament epithelium, (cj) ciliary junction. Malformations (MF), gill epithelium alterations which become highly vacuolated (black arrows), chr chitinous rods, curvature of gill filaments (black arrows), necrotic gill filament (ngf), ciliary erosion (e), epithelial exfoliation (EE), frontal bulge of filaments becomes clop shaped (circle), bd, branchial dymorphia, Ax: gill axis, detached gill epithelium (arrows), haemocytes (h), blocked branchial vessel (*), heamocyte infiltration (hi), thick chitinous layer (arrows), aggregation of brown cells (Brc), gill atrophy (ga) with dwarfism, oedema of the branchial vessel (o)

15 days of exposure (Gomes et al. 2011; 2012). MTs also play a role in oxidative stress because they capture oxidant radicals, such as superoxide and hydroxyl radicals, and this role is most likely suggested in bivalves exposed to NPs (Gomes et al. 2011). This role may be achieved due to the stoichiometry of the MT proteins, which has four metal-binding domains [tetra-domained MT] as discussed by Moreau et al. (2008).

Table 4 Semi-quantitative analysis of the histological alterations in gills of the mussel *L. lithophaga* after exposure to CuO NPs for 4 weeks

Exposure/histopathological changes	Control	5 µg/L	20 µg/L
Necrosis	-	40	80
Malformations of filament tips	-	40	50
Haemocyte infiltration	10	40	50
Epithelial detachment	-	-	40
Ciliary erosion	-	60	70
Blocked branchial vessel	-	-	60
Dilation of branchial vessel	-	60	80
Thickened chitinous sheet	-	-	80
Vacuolization of gill epithelium	-	50	-
Fusion of gill filaments	-	-	50
Brown cell aggregation	-	-	40
Increased interfilamentar spaces	-	50	80
Dwarfism of gill filaments	-	40	80
Oedema	-	40	50
Epithelial exfoliation	-	-	50
Gill atrophy	-	-	50

Note: $n \geq 15$ replicates for the control and exposed mussels. Data were represented as percentage (%) of the total collected sections

SEM of the gills of the mussel *L. lithophaga* exposed to CuO NPs showed shrunken axis edges with several grooves and precipitation of CuO NPs on the axis and the filaments. Changes in the shape of gill filaments were reported as a prime response of *M. edulis* mussels to metal pollution, and it was described as a slacking of the abfrontal and frontal muscles and resultant dilation of the branchial vein (Sunila 1986).

The gills of *L. lithophaga* collected from the exposed group exhibited ciliary erosion, irregular arrangement, vacuolization, fusion and swelling of gill filaments, and disappearance and/or disposition of the ciliary discs. Al-bairuty (2013) indicated that exposure to copper NPs resulted in some increases in the incidence of oedema in the lamellae, lamellar fusion, clubbed tips and necrosis in the lamellae of the gill filaments of rainbow trout. These changes could be signs of NP intake and/or adaptation to avoid the pollutant's entry through the gill filament surface (Olurin et al. 2006). The present study of *L. lithophaga* exposed to CuO NPs revealed a shortening of gill filaments, vacuolated epithelial cells, alterations in cilia, dilation of the branchial vessel and malformation at tips. These results are similar to *Mytella falcate* collected from contaminated areas of the Santos estuary (David and Fontanetti 2005). García-Negrete et al. (2013) observed histopathological lesions in the gill tissues specifically epithelial cells, basal lamina, cilia and microvilli in the apex of the cell of the marine bivalve, *Ruditapes philippinarum*, after short exposures (6 h) to an Au NP solution. They added that these changes may cause an impairment of respiration and feeding. Martín-Díaz et al. (2008) and Ben Khedher et al. (2014) reported histopathological lesions in the gills of the clam, *Ruditapes philippinarum*, such as haemocyte infiltration, lamellar epithelium lifting, necrosis and the fusion of gill lamellae, which was exposed to a mixture of metals. Metals, such as Cu, may affect the microtubule structures of the gills by directly binding to tubulin thiol groups or indirectly inducing alterations of the redox balance and oxidative stress conditions in the tissue (Viarengo et al., 1994). In the present study, inflammation and brown cells were recorded. According to previous studies, inflammatory responses in the gills tend to be nonspecific and reflect a physiological adaptation to any stress (Mallatt 1985). Besides, Bhavan and Geraldine (2000) explained that changes may be a protective mechanism where the vulnerable surface area of the gills is decreased to keep the osmoregulatory functions. This change could be a result of haemocytes moving from the circulation to the tissue for injury repair purposes (Sheir et al. 2013). The presence of brown cells jointly with haemocyte infiltration and hypertrophy confirmed the inflammatory condition of the treated molluscs as mentioned by De Vico and Carella (2012). Moreover, it confirms the aetiology of pathological lesions because these cells participate in the accumulation and detoxification of metabolites and pollutants (Zaroogian et al. 1993; Usheva and Frolova 2006; De Vico and Carella 2012).

Conclusions

The current results highlighted a battery of biomarkers used as a response of *L. lithophaga* to CuO NP impacts. Firstly, immunotoxic impacts were demonstrated via the impairment of the phagocytic activity and the destabilization of the haemocyte membrane. Moreover, the genotoxic effects on DNA integrity of gill cells were investigated. Finally, morphological and histopathological alterations of gill tissue were assessed. Thus, the mussels responded to the concentrations and different time periods of exposure that were selected, rendering this bivalve a potential bioindicator for CuO NP toxicity assessment.

Acknowledgements The authors greatly appreciate the help provided by Professor Dr. Ahmed El-Hamalawy, Prof. of Solid State Physics, Lab. of Renewable Energy (LORE), Faculty of Science, Menoufia University, in the results of CuO nanoparticle characterization.

Author contribution AEE was responsible for the conceptualization, review and supervision of the work.

SSE was responsible for the review, writing of the original draft and supervision of the work.

GYO was responsible for the review, editing and supervision.

RME was responsible for the methodology, analysis, investigations and writing of the original draft.

ASA was responsible for the review of the work.

SKS was responsible for the conceptualization, methodology, validation, investigations, resources, writing of the original draft, editing, visualization and supervision of the work.

Funding The current study was funded personally by the authors.

Data availability Data are available.

Declarations

Ethics approval No ethical approval is needed for invertebrate animals (bivalves) according to the IACUC approval sheet.

Consent to participate Not applicable.

Consent to publication Not applicable.

Competing interests The authors declare no competing interests.

References

Abdul-Salam JM, Michelson IEH (1980) Phagocytosis by amoebocytes of *Biomphalaria glabrata*: absence of opsonic factor. Malacol Rev 13:81–83

Al-bairuty GA (2013) Histopathological effects of metal and metallic nanoparticles on the body systems of rainbow trout (*Oncorhynchus mykiss*). Dissertation, University of Plymouth

Almeida JC, Cardoso CED, Pereira E, Freitas R (2019) Toxic effects of metal nanoparticles in marine invertebrates. In: Gonçalves G, Marques P (Eds) Nanostructured materials for treating aquatic pollution. Engineering Materials. Springer, Cham, Switzerland, pp175–224.

Alnashiri HM (2015) The ecotoxicology of different forms of copper (nano and micro and salt) in marine mussels. Dissertation, Heriot-Watt University -Edinburgh, Scotland, United Kingdom.

Amiard JC, Amiard-Triquet A, Barka S, Pellerin S, Rainbow PS (2006) Metallothioneins in aquatic invertebrates: their role in metal detoxification and their use as biomarkers. Aquat Toxicol 76:160–202

Anyaogu KC, Fedorov AV, Neckers DC (2008) Synthesis, characterization, and antifouling potential of functionalized copper nanoparticles. Langmuir 24(8):4340–4346

Babich H, Borenfreund E (1992) Neutral red assay for toxicology in vitro. In: Watson RR (ed) In vitro methods of toxicology. CRC Press, Boca Raton, Florida, pp 237–251

Ben Khedher S, Jebali J, Houas Z, Nawei H, Jrad A, Banni M, Boussetta H (2014) Metals bioaccumulation and histopathological biomarkers in Carcinus maenas crab from Bizerta lagoon. Tunisia Environ Sci Pollut Res 21:4343–4357

Bhavan PS, Geraldine P (2000) Histopathology of the hepatopancreas and gills of the prawn *Macrobrachium malcolmsonii* exposed to endosulfan. Aquat Toxicol 50:331–339

Canesi L, Corsi I (2016) Effects of nanomaterials on marine invertebrates. Sci Total Environ 565:933–940

Canesi L, Ciacci C, Fabbri R, Marcomini A, Pojana G, Gallo G (2012) Bivalve molluscs as a unique target group for nanoparticle toxicity. Mar Environ Res 76:16–21

Canesi L, Ciacci C, Vallotto D, Gallo G, Marcomini A, Pojana G (2010) In vitro effects of suspensions of selected nanoparticles (C60 fullerene, TiO2, SiO2) on *Mytilus* hemocytes. Aquat Toxicol 96:151–158

D'Angelo, G., Gargiullo, S., 1978. Guida alle conchigle Mediterranee. Gruppo Editore Fabbri, Milano. 224.

Dasari TP, Pathakoti K, Hwang HM (2013) Determination of the mechanism of photoinduced toxicity of selected metal oxide nanoparticles (ZnO, CuO, Co3O4 and TiO2) to E. coli bacteria. J. Environ. Sci. 25(5):882–888

David JAO, Fontanetti CS (2005) Surface morphology of *Mytella falcata* gill filaments from three regions of the Santos estuary. Braz J Morphol Sci 22(4):203–210

Devescovi M (2009) Biometric differences between date mussels *Lithophaga lithophaga* colonizing artificial and natural structures. Acta Adriatica. Int J Mar Sci 50:129–138

De Vico G, Carella F (2012) Morphological features of the inflammatory response in molluscs. Res Vet Sci 93:1109–1115

Dufour SC, Beninger PG (2001) A functional interpretation of cilia and mucocyte distributions on the abfrontal surface of bivalve gills. Mar Biol 138(2):295–309

Felgenhauer B (1987) Techniques for preparing crustaceans for scanning electron microscopy. J Crust Biol 7:71–76

Federici G, Shaw BJ, Handy RD (2007) Toxicity of titanium dioxide nanoparticles to rainbow trout (*Oncorhynchus mykiss*): gill injury, oxidative stress, and other physiological effects. Aquat Toxicol 84:415–430

Ghadimi M, Zangenehtabar S, Homaeigohar S (2020) An overview of the water remediation potential of nanomaterials and their ecotoxicological impacts. Water 12(4):1150

Gagné F, Auclair J, Turcotte P (2008) Ecotoxicity of Cd Te quantum dots to freshwater mussels: impacts on immune system, oxidative stress and genotoxicity. Aquat Toxicol 86(3):333–340

Galinou-Mitsoudi S, Sinis AI (1995) Age and growth of *Lithophaga lithophaga* (Linnaeus, 1758) (Bivalvia: Mytilidae), based on annual growth lines in the shell. J Mollus Stud 61:435–453

García-Negrete CA, Blasco J, Volland M, Rojas TC, Hampel M, Lapresta-Fernández A, Jiménez de Haro MC, Soto M, Fernández A (2013) Behaviour of Au-citrate nanoparticles in seawater and accumulation in bivalves at environmentally relevant concentrations. Environ Pollut 174:134–141

Gomes T, Araújo O, Pereira R, Almeida AC, Cravo A, Bebianno MJ (2013) Genotoxicity of copper oxide and silver nanoparticles in the mussel *Mytilus galloprovincialis*. Mar Environ Res 84:51–59

Gomes T, Chora S, Pereira CG, Cardoso C, Bebianno MJ (2014a) Proteomic response of mussels *Mytilus galloprovincialis* exposed to CuO NPs and Cu^{2+}: an exploratory biomarker discovery. Aquat Toxicol 155:327–336

Gomes T, Pereira CG, Cardoso C, Sousa VS, Teixeira MR, Pinheiro JP, Bebianno MJ (2014b) Effects of silver nanoparticles exposure in the mussel *Mytilus galloprovincialis*. Mar Environ Res 101:208–214

Gomes T, Pereira CG, Cardoso C, Pinheiro JP, Cancio I, Bebianno MJ (2012) Accumulation and toxicity of copper oxide nanoparticles in the digestive gland of *Mytilus galloprovincialis*. Aquat Toxicol 118–119:72–79

Gomes T, Pinheiro JP, Cancio I, Catarina G, Pereira CG, Cardoso C, Bebianno MJ (2011) Effects of copper nanoparticles exposure in the mussel *Mytilus galloprovincialis*. Environ Sci Technol 45:9356–9362

Gonzalez, J.T., Halcon, R.M.A., Barrajon, A., Calvo, M., Frias, A., Morreno, D., Saavedra, L., 2000. Estudio sobre la biologia, conservacio´ny problema´tica del da´til de mar (*Lithophaga lithophaga*) en Espana. Madrid, Ministerio de Medio Ambiente, Direccio´n General de Conservacio´n de la Naturaleza 66.

Gunawant C, Teoh WY, Marquis CP, Amal R (2011) Cytotoxic origin of copper (II) Oxide nanoparticles: comparative studies with

micron-sized particles, leachate, and metal salts. ACS Nano 5:7214–7225
Holsapple MP, Farland WH, Landry TD, Monteiro-Riviere NA, Carter JM, Walker NJ, Thomas KV (2005) Research strategies for safety evaluation of nanomaterials, part II: toxicological and safety evaluation of nanomaterials, current challenges and data needs. Toxicol Scie 88(1):12–17
Hu W, Culloty S, Darmody G, Lynch Davenport S, Ramirez-Garcia S, Dawson KA, Lynch I, BlascoSheehan JD (2014) Toxicity of copper oxide nanoparticles in the blue mussel, *Mytilus edulis*: a redox proteomic investigation. Chemosphere 108:289–299
Katsumiti A, Thorley AJ, Arostegui I, Reip P, Valsami-Jones E, Tetley TD, Cajaraville MP (2018) Cytotoxicity and cellular mechanisms of toxicity of CuO NPs in mussel cells in vitro and comparative sensitivity with human cells. Toxicol Vitro 48:146–158
Koffyberg FP, Benko FA (1982) A photoelectrochemical determination of the position of the conduction and valence band edges of p-type CuO. J Appl Phys 53:1173–1177
Koehler A, Marx U, Broeg K, Bahns S, Bressling J (2008) Effects of nanoparticles in *Mytilus edulis* gill and hepatopancreas – a new threat to marine life. Mar Environ Res 66:12–14
Liu Z, Wu Y, Guo Z, Liu Y, Shen Y, Zhou P, Lu X (2014) Effects of internalized gold nanoparticles with respect to cytotoxicity and invasion activity in lung cancer cells. PLoS One. 9(6):e99175
Lowe DM, Fossato VU, Depledge MH (1995) Contaminant-induced lysosomal membrane damage in blood cells of mussels *Mytilus galloprovincialis* from the Venice Lagoon: an in vitro study. Mar Ecol Prog Ser 129:189–196
Luengen AC, Friedman CS, Raimondi PT, Flegal AR (2004) Evaluation of mussel immune responses as indicators of contamination in San Francisco Bay. Mar Environ Res 57:197–212
Luoma SN, Rainbow PS (2005) Why is metal bioaccumulation so variable? Biodynamics as a unifying concept. Environ Sci Technol 39:1921–1931
Mallatt J (1985) Fish gill structural changes induced by toxicants and other irritants: a statistical review. Can J Fish Aquat Sci 42:630–648
Marquis BJ, Love SA, Braun KL, Haynes CL (2009) Analytical methods to assess nanoparticle toxicity. Analyst 134:425–439
Martín-Díaz ML, Jiménez-Tenorio N, Sales D, Delvalls TA (2008) Accumulation and histopathological damage in the clam *Ruditapes philippinarum* and the crab *Carcinus maenasto* assess sediment toxicity in Spanish ports. Chemosphere 71:1916–1927
Moore MN (2006) Do nanoparticles present ecotoxicological risks for the health of the aquatic environment? Environ Int 32:967–976
Moreau JL, Baudrimont M, Carrier P, Peltier G, Bourdineaud JP (2008) Metal binding and antioxidant properties of chimeric triand tetradomained metallothioneins. Biochimie 90:705–716
Mortimer M, Kasemets K, Kahru A (2010) Toxicity of ZnO and CuO nanoparticles to ciliated protozoa *Tetrahymena thermophila*. Toxicology 269(2–3):182–189
Mouneyrac C, Buffet PE, Poirier L, Zalouk-Vergnoux A, Guibbolini M, Faverney CR, Gilliland D, Berhanu D, Dybowska A, Châtel A, PerreinEttajni H, Pan JF, Thomas-Guyon H, Reip P, Valsami-Jones E (2014) Fate and effects of metal-based nanoparticles in two marine invertebrates, the bivalve mollusk *Scrobicularia plana* and the annelid polychaete *Hediste diversicolor*. Environ Sci Pollut Res 21:7899–7912
Nessim RB, Salem DMSA, Abdel Ghani SAH, Abou-Taleb AEA (2010) Level of some major constituents of the Egyptian Mediterranean Coastal waters. Egypt J Aquat Res 36:1–9
Okbah MA, Nasr SM, Soliman NF, Khairy MA (2014) Distribution and contamination status of trace metals in the Mediterranean coastal sediments. Egypt Soil Sed Contam 23:656–676
Olurin K, Olojo E, Mbaka G, Akindele A (2006) Histopathological responses of the gill and liver tissues of *Clarias gariepinus* fingerlings to the herbicide, glyphosate. Afr J Biotechnol 5:2480–2487
Rocha TL, Gomes T, Sousa VS, Mestre NC, Bebianno MJ (2015) Ecotoxicological impact of engineered nanomaterials in bivalve molluscs: an overview. Mar Environ Res 111:74–88
Romeis, B., 1989. Mikroskopische Technik, 17 Auflage, Urban & Schwarzenberg, München– Wien – Baltimore.
Riisgård HU, Funch P, Larsen PS (2015) The mussel filter–pump–present understanding, with a re-examination of gill preparations. Acta Zoo 96:273–282
Ruiz P, Katsumiti A, Nieto JA, Bori J, Jimeno-Romero A, Reip P, Arostegui I, Orbea A, Cajaraville MP (2015) Short-term effects on antioxidant enzymes and long-term genotoxic and carcinogenic potential of CuO nanoparticles compared to bulk CuO and ionic copper in mussels *Mytilus galloprovincialis*. Mar Environ Res 111:107–120
Sheir SK, Handy RD (2010) Tissue injury and cellular immune responses to cadmium chloride exposure in the common mussel *Mytilus edulis*: modulation by lipopolysaccharide. Arch Environ Contam Toxicol 59:602–613
Sheir SK, Handy RD, Henry TB (2013) Effect of pollution history on immunological responses and organ histology in the marine mussel *Mytilus edulis* exposed to cadmium. Arch Environ Contam Toxicol 64:1–170
Singh CR, Kathiresan K, Anandhan S (2015) A review on marine based nanoparticles and their potential applications. Afr J Biotech 14(18):1525–1532
Singh NP, McCoy MT, Tice RR, Schneider EL (1988) A simple technique for quantitation of low-levels of DNA damage in individual cells. Exp Cell Res 175:184–191
Sunila I (1986) Chronic histopathological effects of short term copper and cadmium exposure on the gill of the mussel, *Mytilus edulis*. J Invert Pathol 47:125–142
Tedesco S, Doyle H, Redmond G, Sheehan D (2008) Gold nanoparticles and oxidative stress in Mytilus edulis. Mar Environ Res 66(1):131–133
Tsunekawa S, Fukuda T, Kasuya A (2000) Blue shift in ultraviolet absorption spectra of monodisperse CeO 2–x nanoparticles. J Appl Phys 87:1318–1321
Usheva LN, Frolova LT (2006) Morphofunctional changes of the digestive gland in the bivalve mollusk *Crenomytilus grayanus* (Dunker, 1853) in normal conditions and after parasitic invasion by trematodes. Russ J Mar Biol 32:96–105
Van Den Brink NW, Kokalj AJ, Silva PV, Lahive E, Norrfors K, Baccaro M, Khodaparast Z, Loureiro S, Drobne D, Cornelis G, Lofts S (2019) Tools and rules for modelling uptake and bioaccumulation of nanomaterials in invertebrate organisms. Environ Sci Nano 6:1985–2001
Van OR, Porte-Visa C, Van den Brink NW (2005) Ecotoxicological testing of marine and freshwater ecosystems. In: Munawar M, Den Besten PJ (eds) Biomarkers in environmental assessment. Taylor and Francis, Boca Raton, pp 87–152
Viarengo A, Arena N, Canesi L, Alia FA, Orunesu M (1994) Structural and biochemical alterations in the gills of copper exposed mussels. In: Renzoni A, Mattei N, Lari L (eds) Contaminants in the environment. Lewis Publishers, Boca Raton, pp 135–144
Viarengo A, Ponzano E, Dondero F (1997) A simple spectrophotometric method for metallothionein evaluation in marine organisms: an application to Mediterranean and Antarctic Molluscs. Mar Environ Res 44:69–84
Zaroogian G, Yevich P, Anderson S (1993) Effect of selected inhibitors on cadmium, nickel and benzo [a] pyrene uptake into brown cells of Mercenaria mercenaria. Mar Environ Res 35:41–45

Zha S, Rong J, Guan X, Tang Y, Han Y, Liu G (2019) Immunotoxicity of four nanoparticles to a marine bivalve species, *Tegillarca granosa*. J Hazard Mater 377:237–248

Zhu H, Han D, Meng Z, Wu D, Zhang C (2011) Preparation and thermal conductivity of CuO nanofluid via a wet chemical method. Nanoscale Res Lett 6:181